https://doi.org/10.5194/esd-2020-84
Preprint. Discussion started: 26 November 2020

Earth System Dynamics Discussions

Climate Change Projections of Terrestrial Primary Productivity over the Hindu Kush Himalayan Forests

Halima Usman[1], Thomas A.M. Pugh[2], Anders Ahlström[3], Sofia Baig[1*]

[1]Institute of Environmental Sciences & Engineering, National University of Sciences and Technology, Islamabad, 44000, Pakistan

[2]School of Geography, Earth and Environmental Sciences, University of Birmingham, Edgbaston, Birmingham, B15 2TT, UK

[3]Department of Physical Geography and Ecosystem Science, Lund University, Lund, SE-221 00, Sweden

Correspondence to: Sofia Baig (e-mail: sofia.baig@iese.nust.edu.pk)

Abstract. Increasing atmospheric carbon dioxide concentration [CO_2] caused by anthropogenic activities has triggered a requirement to predict the future impact of [CO_2] on forests. The Hindu Kush Himalayan (HKH) region comprises a vast territory including forests, grasslands, farmlands and wetland ecosystems. In this study, the impacts of climate change and land use change on forest carbon fluxes and vegetation productivity are assessed for HKH using the Lund-Potsdam-Jena General Ecosystem Simulator (LPJ-GUESS). LPJ-GUESS simulations were driven by an ensemble of three climate models participating in the CMIP5 (Coupled Model Intercomparison Project Phase 5) database. The modeled estimates of vegetation carbon (VegC) and terrestrial primary productivity were compared with observation-based estimates. Furthermore, we also explored the net biome productivity (NBP) and VegC over HKH for the period 1850-2100 under the future climate scenarios RCP2.6 and RCP8.5. A reduction is observed in modeled NBP and VegC from 1951-2005 primarily due to land use change. However, an increase in both NBP and VegC is predicted under RCP2.6 and RCP8.5. The findings of the study have important implications for management of the HKH region and inform strategic decision making, land use planning and clarify policy concerns.

1 Introduction

Anthropogenic activities such as combustion of fossil fuels and land use changes have led to large rises in atmospheric greenhouse gas (GHG) emissions such as carbon dioxide (CO_2) and methane over the last century, with atmospheric CO_2 mixing ratios increasing from 280 to 407.38±0.1 ppm in 2018 since the preindustrial period, and presently rising at the mean rate of 1.9 ppm per year (Friedlingstein et al., 2019). Terrestrial ecosystems aid mitigation of climate change by absorbing anthropogenic CO_2 emissions, taking up 3.5Gt C in 2018 (Friedlingstein et al., 2019). This uptake is likely primarily driven by the fertilizing effects of elevated atmospheric CO_2 concentrations on plant growth (Sitch et al., 2015) and by the regrowth of forests following past disturbances (Kondo et al., 2018; Pugh et al., 2019) . However, the ability of this land sink to continue in the future remains highly uncertain (Phillips and Lewis, 2014). Several studies have identified that warming can cause a stimulation in plant growth by increasing NPP and hence leading to enhanced carbon uptake (Delpierre et al., 2009;Sullivan et al., 2008;Wu et al., 2011). However, researchers

https://doi.org/10.5194/esd-2020-84
Preprint. Discussion started: 26 November 2020


Earth System Dynamics Discussions Open Access EGU

have also addressed that the rising air temperatures may also stimulate autotrophic respiration in plants(Burton J. Andrew et al., 2008). Due to global temperature rise, droughts are predicted to increase in frequency, duration and severity in the future (Trenberth et al., 2013). Increase in temperature causes an exponential rise vapor pressure deficit resulting in stomatal closure thus limiting the rate of photosynthesis and higher mortality (Williams et al., 2013). Hence, the determination of the effect of global rise in temperature on forests is becoming increasingly important as vegetation response to climate change will result in changes in net carbon uptake, water use efficiency, plant establishment, carbon biomass allocation and response to disturbances (Urban et al., 2017). Several publications have appeared in recent years, showing that climate warming and increases in atmospheric CO_2 concentration are expected to lead to large increases in ecosystem carbon storage at the global scale throughout the 21st century Ahlström et al., 2012; Pugh et al., 2018; Todd-Brown et al., 2014).

The HKH region is a significant, diverse and ecological buffer zone, often referred to as the "Third Pole" encompassing an area of 4.2 million km^2 and is surrounded by eight countries. The region provides unique ecosystem services sustaining communities of estimated 240 million people (Krishnan et al., 2019). Over the past 100 years, the rate of warming is significantly higher than the global average of 0.74°C in the HKH region (Du et al., 2004). Since 1960, the HKH has been experiencing temperature rise of 0.2°C per decade since 1960 (Chen et al., 2013). The forests of HKH are undergoing changes of various intensity due to climatic and human disturbances, and various forest management policies practiced by the different countries occupying the region (Behera et al., 2018; Das et al., 2017). The rate of deforestation along the HKH has been reported to be 0.5% in Bhutan and 1.7% in Myanmar (Chettri et al., 2019). The warming trend observed over recent decades of the 20th century is attributed to the increase in anthropogenic greenhouse gas (GHG) concentrations. HKH region is believed to become increasingly sensitive to climate change (Krishnan et al., 2019). In this region, the carbon dynamics is mostly influenced by the combined effects of climatic change and land use land cover change (LULCC) (Almeida et al., 2018;Cao et al., 2018) . Although research has illuminated the projected changes of temperature due to climate change in the countries in the locality of HKH, little is known about the effect of long-term influence of increasing [CO_2] and land use change primarily on the vegetation productivity.

In this paper, the historical and future carbon balance of terrestrial ecosystems in the HKH region are investigated using results from the Lund-Potsdam-Jena General Ecosystem Simulator (LPJ-GUESS), a DGVM with a detailed description of forest stand structure and land use (Ahlström et al., 2012; Smith et al., 2001). The goal of the present study is to (1) evaluate the ability of the LPJ-GUESS model, as forced by climate from a selection of Global Climate Models, to reproduce observation-based estimates of vegetation carbon and satellite-derived estimates of gross primary productivity (GPP) and net primary productivity (NPP) and (2) analyze the spatial and temporal changes in net biome productivity (NBP) and vegetation carbon storage (VegC) over the period 1850-2100.

https://doi.org/10.5194/esd-2020-84
Preprint. Discussion started: 26 November 2020

Earth System Dynamics Discussions
Open Access
EGU

2 Materials and Methods

2.1 Study Area

The HKH region is situated between 16°N–40°S and 61–105°E encompassing Afghanistan, Bangladesh, Bhutan, China, India, Myanmar, Nepal and Pakistan (Figure 1). The evergreen needleleaf forest (ENF) cover about 2.69% of the HKH and 10.5%, 0.06%, 1.09%, 9.37% is covered by evergreen broadleaf forest (EBF), deciduous needleleaf forest (DNF), deciduous broadleaf forest (DBF) and mixed forests (MF) respectively. A major percentage of landcover is covered by open shrublands (OShrub) and grasslands (Grass) occupying 31.57% and 32.08% of the area of HKH. Furthermore, savannas (Sav) and woody savannas (Wsav) cover about 1.19% and 4.46% respectively. The remaining land is covered by croplands (Crop) and closed shrubland (CShrub) with percentage of 5.61% and 1.09% respectively. The forests of the HKH cover about 24% of the region, supporting the 12% of the population of the world by provision of diverse ecosystem goods and ecosystem services including energy, timber and freshwater (Behera et al., 2018)

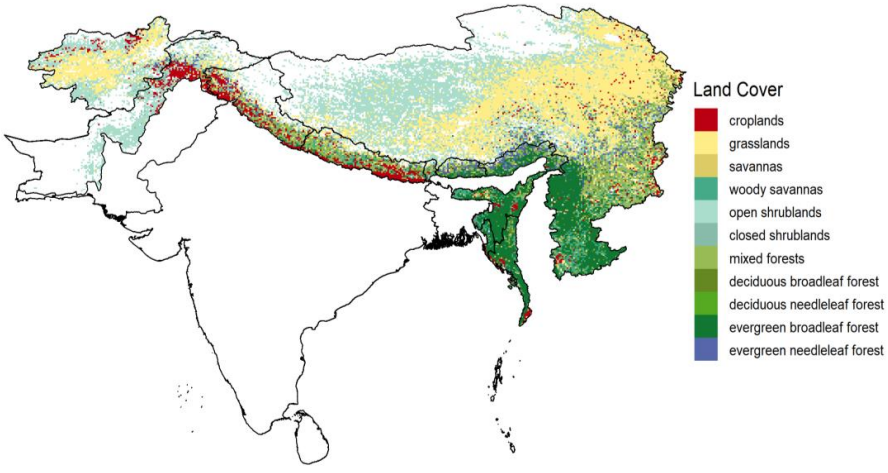

Figure 1: Land cover of HKH from MODIS (MOD12Q1).

2.2 LPJ-GUESS Ecosystem Model

LPJ-GUESS is a coupled biogeography-biogeochemistry model which integrates process-based representation of terrestrial vegetation dynamics and biogeochemical cycling (Smith et al., 2001). In order to simulate the size of carbon pools in various parts of the plant such as leaves, sapwood, litter and soil the model explicitly takes account of processes such as photosynthesis, allocation and resource competition between plants. The model is useful for predicting the changes in the ecosystem dynamics and is able to simulate and predict the future response of vegetation to elevated CO_2 levels at leaf and stand scales (Sitch et al., 2015). In LPJ-GUESS, the species diversity of terrestrial vegetation is represented as groups of species with analogous traits known as Plant Functional Types (PFTs). The

https://doi.org/10.5194/esd-2020-84
Preprint. Discussion started: 26 November 2020

simulations here use ten PFTs that are differentiated by attributes such as physiology, morphology, phenology and response to disturbance along with bioclimatic constraints. Trees are modelled as age cohorts across multiple replicate patches, but are identical within each cohort (age class) (Smith et al., 2001).

LPJ-GUESS works on a daily time steps, with some processes, such as vegetation dynamics, computed annually. The input data to the model includes atmospheric [CO_2] mixing ratio, precipitation, shortwave radiation, air temperature and soil type. Simulations begin from bare ground, and go through a 500 year "spin-up phase" during which soil and carbon litter pools accumulate and reach a state of equilibrium. An analytical solution is used to accelerate spin-up of the soil carbon pools. In the spin-up phase the model is forced by constant [CO_2] and a repeated detrended 30-year climate segment from the beginning of the climate dataset used. As the spin-up phase finishes, the "transient phase" begins, in which land use, climate and [CO_2] evolve over time as specified in the forcing datasets. Here we analyze outputs of vegetation carbon, gross primary productivity, net primary productivity and net biome productivity.

2.3 Simulation Protocol

In this study simulations are reanalyzed from (Ahlström et al., 2012) with a focus on the HKH region. Only an overview of the salient features of the set-up are given for this study. For more set-up details, please see (Ahlström et al., 2012). Spatial patterns of carbon pool, fluxes and terrestrial primary productivity were investigated in HKH forests by using the output simulations of LPJ-GUESS resolution of 0.5° × 0.5° with climate forcing from three climate models participating in CMIP5 (Table 1) under RCP 2.6 (Van Vuuren et al., 2007) and RCP8.5 representative concentration pathway (Riahi et al., 2011). RCP2.6 emission pathway is representative of scenarios indicating to extremely reduced GHG concentration levels. It is a defined as a "peak-and-decline" scenario, in which the radiative forcing level first reaches around 3.1 W/m^2 by mid-century, and return to a value of 2.6 W/m^2 by 2100. In contrast, RCP8.5 is characterized by increasing GHG emissions over time, culminating in a radiative forcing of 8.5 W/m^2 in 2100. The radiative forcing in RCP 8.5 corresponds approximately to the A2 scenario used in the earlier Special Report on Emission Scenarios (SRES) (Stocker et al., 2013).

Croplands and pastures were correspondingly treated as natural grasslands in the vegetation model (Ahlström et al., 2012). The fractional cover of the land use for the historical and scenario period employed by Ahlström et al. (2012) was obtained from the data set of Hurtt et al. (2011). The simulations start from 1850 and end at 2100. The data of the three ESMs was acquired from CMIP5 repository (of April 2012) for which complete series of historical and scenario data were provided (Table 1).

The model output was driven by gridded monthly data for air temperature and precipitation from Climate Research Unit (CRU) Time Series version 3. The climatic data was bias corrected by using CRU TS 3.0 1961-90 climatologies on annual and monthly basis (seasonal bias correction), the monthly fields of precipitation, downward shortwave radiation and air temperature were bi-linearly interpolated to the CRU grid at a resolution of 0.5°x0.5°. The correction in the climatology field (1961-90) adjust for biasness and annual averages and seasonal distribution.

https://doi.org/10.5194/esd-2020-84
Preprint. Discussion started: 26 November 2020

Earth System Dynamics Discussions

Modelling Center	Institute ID	Model name
National Center for Atmospheric Research	NCAR	CCSM4
Institut Pierre–Simon Laplace	IPSL	IPSL-CM5A-MR
Max Planck Institute for Meteorology	MPI-M	MPI-ESM-LR

Table 1: CMIP5 models and modelling groups used to provide climate forcing data for LPJ-GUESS in this study.

2.4 Model Evaluation

In this study, a global dataset of forest above-ground biomass (AGB) developed within European Commission-funded GEOCARBON project was considered for the purpose of comparison with LPJ-GUESS VegC. The base year of this dataset is 2000. As LPJ-GUESS VegC includes both above- and below-ground vegetation carbon, the AGB of GEOCARBON was converted into VegC by applying a correction to estimate below-ground biomass in the GEOCARBON dataset based on (Saatchi et al., 2011). Biomass was converted to carbon by multiplying by 0.5.

Furthermore, the Moderate-resolution Imaging Spectroradiometer (MODIS) GPP and NPP product (MOD17A3H) was used for comparison with the modelled GPP and NPP. MOD17 is based on the light use efficiency approach and consists of two products, MOD17A2 and MOD17A3 (Zhao and Running, 2010). In this study we incorporated MOD17A3 that contains annual sums of GPP and NPP with a 0.0083◦ × 0.0083◦ spatial resolution for the period 2000–2010. In order to compare LPJ-GUESS GPP and NPP estimates, MOD17A3 GPP and NPP datasets were downloaded from "The Application for Extracting and Exploring Analysis Ready Samples (AρρEEARS)" website ("LP DAAC - AppEEARS".). Land cover (MOD12Q1) used in this study was downloaded from files.ntsg.umt.edu/data/NTSG_Products/MOD17/GeoTIFF/MOD12Q1/ and was used for land cover stratification (Friedl et al., 2002). Land cover related to barren, water and urban were masked from LPJ-GUESS data in order to make it comparable with MOD17A3 data (i.e. identical spatial extent, land cover classes and number of grid cells). Both GEOCARBON and MODIS datasets were aggregated to 0.5° x 0.5° resolution for comparison with LPJ-GUESS.

https://doi.org/10.5194/esd-2020-84
Preprint. Discussion started: 26 November 2020

Earth System Dynamics
Discussions
Open Access
EGU

3 Results

3.1 Comparison between Observed and LPJ-GUESS estimations of VegC

Simulations forced by three CMIP5 Earth System Models (ESMs) of mean VegC from 1990-2015 were compared with the observed GEOCARBON dataset (Figure 2). The mean VegC of observed dataset was estimated to be 4.68 kg C m^{-2}. While the modeled VegC for HKH averages 1.92 kg C m^{-2}, 2.04 kg C m^{-2} and 2.11 kg C m^{-2} for simulations forced by climate outputs from IPSL-CM5A-MR, MPI-ESM-LR and CCSM4 respectively. Most of the difference is found to be the southern regions of HKH A moderate agreement was found between the GEOCARBON and LPJ-GUESS VegC with a mean r^2 value of 0.44.

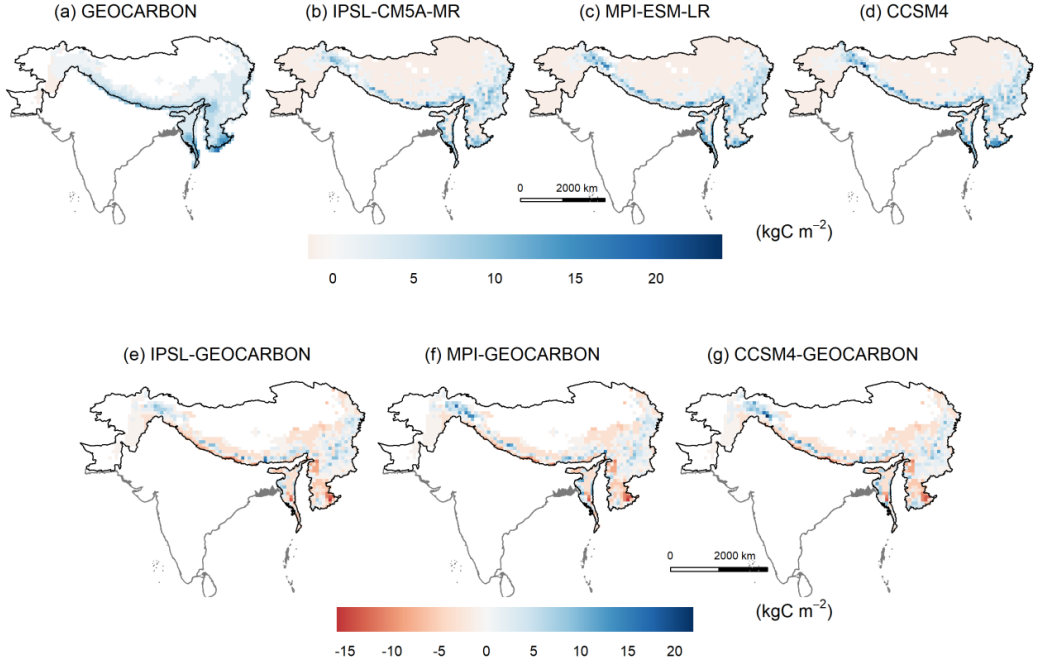

Figure 2: The distribution of VegC as simulated by (a) GEOCARBON, (b) IPSL-CM5A-MR, (c) MPI-ESM-LR (d) CCSM4 and (e,f,g) their respective differences with GEOCARBON dataset for the HKH region.

Furthermore the simulations of the CMIP5 models and the observed estimations in the HKH region were compared according to land cover classes from MOD12Q1 (Figure 3). There is a large overestimation of VegC in evergreen broadleaf forests. The mean GEOCARBON VegC was 7.73 kg C m^{-2} was on average, 2.68 kg C m^{-2} higher than LPJ-GUESS VegC for evergreen broadleaf forest. Overestimation was also observed in grasslands and open shrublands. VegC for remaining forest types showed a lesser difference than 1.5 kg C m^{-2}. It is important to note that the simulation of VegC in not very sensitive to differences in the modelled climates from the CMIP5 models for the period from 1990-2015.

https://doi.org/10.5194/esd-2020-84
Preprint. Discussion started: 26 November 2020

Earth System Dynamics
Discussions
Open Access
EGU

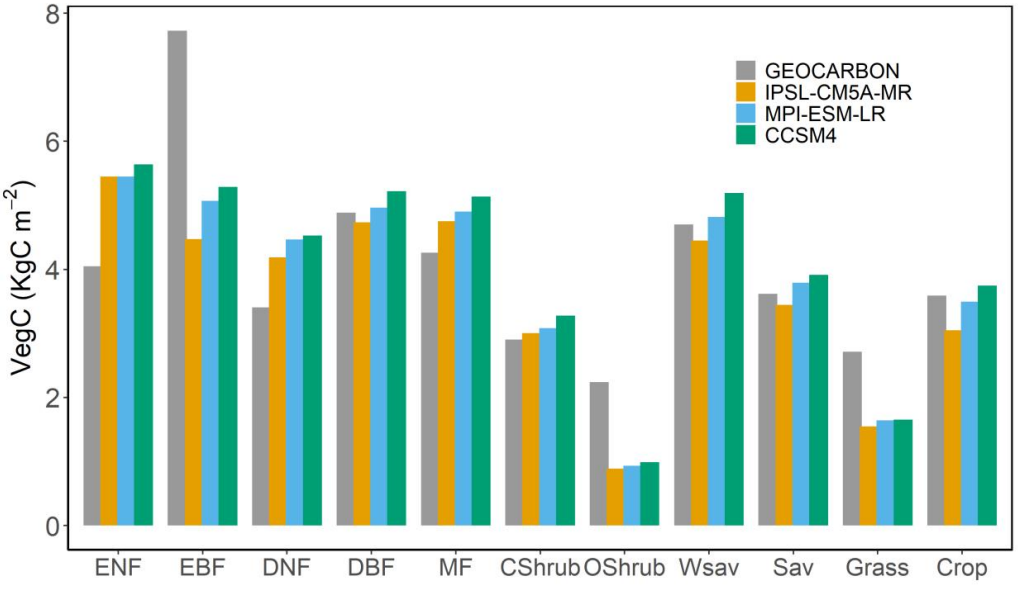

Figure 3: Summary statistics of LPJ-GUESS and GEOCARBON VegC for HKH in KgC m^{-2} of CMIP5 models according to landcover classes

3.2 Evaluation of patterns of GPP and NPP from 2000-2010

The mean MODIS GPP for 2000-2010 was estimated to be 0.69 ± 0.26 kgC m^{-2} yr^{-2}. The GPP for IPSL-CM5A-MR, MPI-ESM-LR and CCSM4 was 0.84 ± 0.17 kgC m^{-2} yr^{-1}, 0.83 ± 0.16 kgC m^{-2} yr^{-1} and 0.88 ± 0.16 kgC m-^{2} yr^{-1} respectively (Figure 4). The mean MODIS NPP was estimated to be 0.40 ± 0.16 kgC m-^{2} yr^{-1} and 0.43 ± 0.07 kgC m-^{2} yr^{-1}, 0.42 ± 0.07 kgC m-^{2} yr^{-1}, and 0.44 ± 0.07 kgC m-^{2} yr^{-1} for IPSL-CM5A-MR, MPI-ESM-LR and CCSM4 respectively (Figure 4). Both of the spatial datasets are able to capture important features such as the low productive Himalayan tundra ecosystem in the north and high productive regions like the forests and croplands in lower parts of HKH region (Figure 5 & 6). There was a moderate spatial agreement between the MODIS and modelled GPP with mean r^2 values of 0.54. However, there was a weak correlation between the satellite-derived and modelled NPP with mean r^2 values of 0.4. A difference is yet again found in the EBF land cover class when both datasets are compared (Figure 7a, 7b).

https://doi.org/10.5194/esd-2020-84
Preprint. Discussion started: 26 November 2020

Earth System Dynamics
Discussions
Open Access
EGU

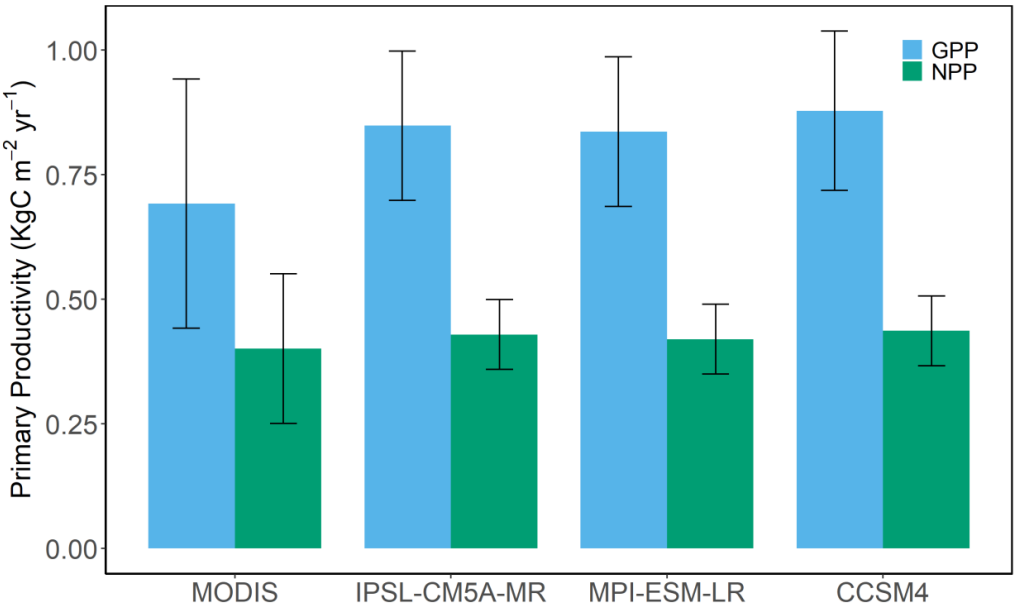

Figure 4: GPP and NPP for HKH showing mean GPP (blue) and mean NPP (green) from MOD17 and from the LPJ-GUESS model (average for the period 2000–2010). Vertical black bars illustrate ± standard error where *n*=11

https://doi.org/10.5194/esd-2020-84
Preprint. Discussion started: 26 November 2020

Earth System Dynamics
Discussions
Open Access
EGU

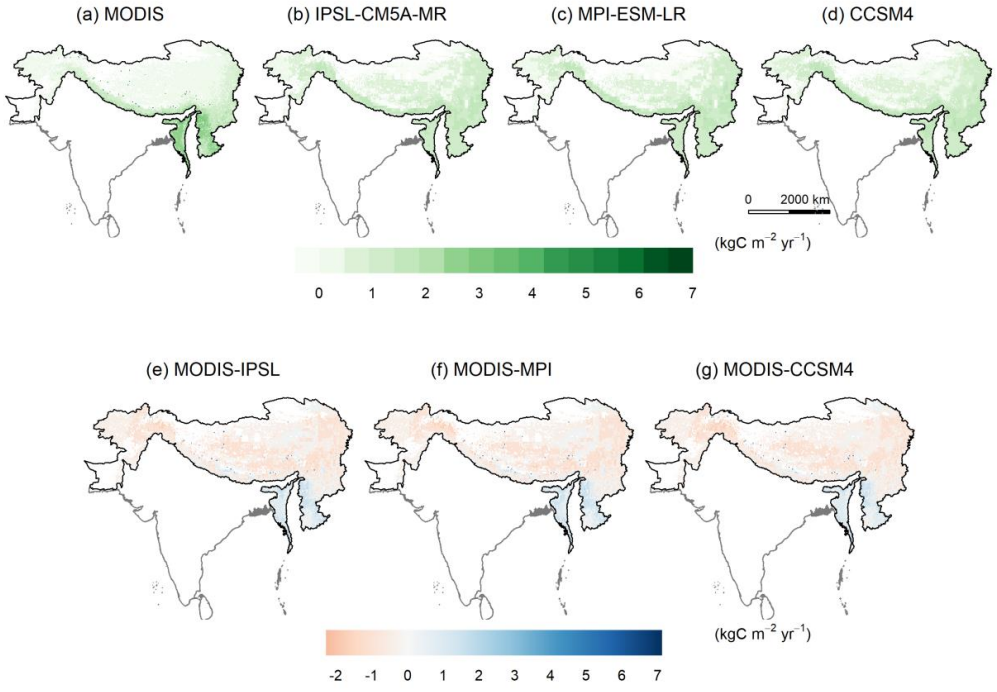

Figure 5: Mean GPP output simulations from 2000 and 2010 of (a) MODIS, (b) IPSL-CM5A-MR, (c) MPI-ESM-LR and (d) CCSM4 and (e, f, g) difference between MODIS and LPJ-GUESS simulations

https://doi.org/10.5194/esd-2020-84
Preprint. Discussion started: 26 November 2020

Earth System Dynamics
Discussions
Open Access
EGU

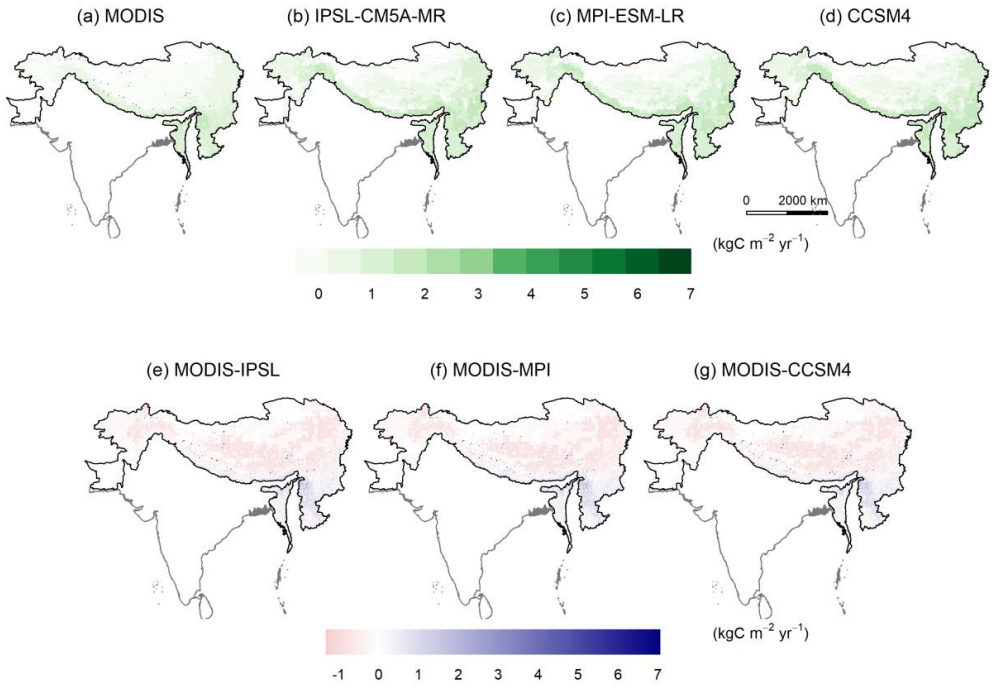

195

Figure 6: Mean NPP output simulations from 2000 and 2010 of (a) MODIS, (b) IPSL-CM5A-MR, (c) MPI-ESM-LR and (d) CCSM4 and (e, f, g) difference between MODIS and LPJ-GUESS simulations.

https://doi.org/10.5194/esd-2020-84
Preprint. Discussion started: 26 November 2020

Earth System Dynamics
Discussions
Open Access
EGU

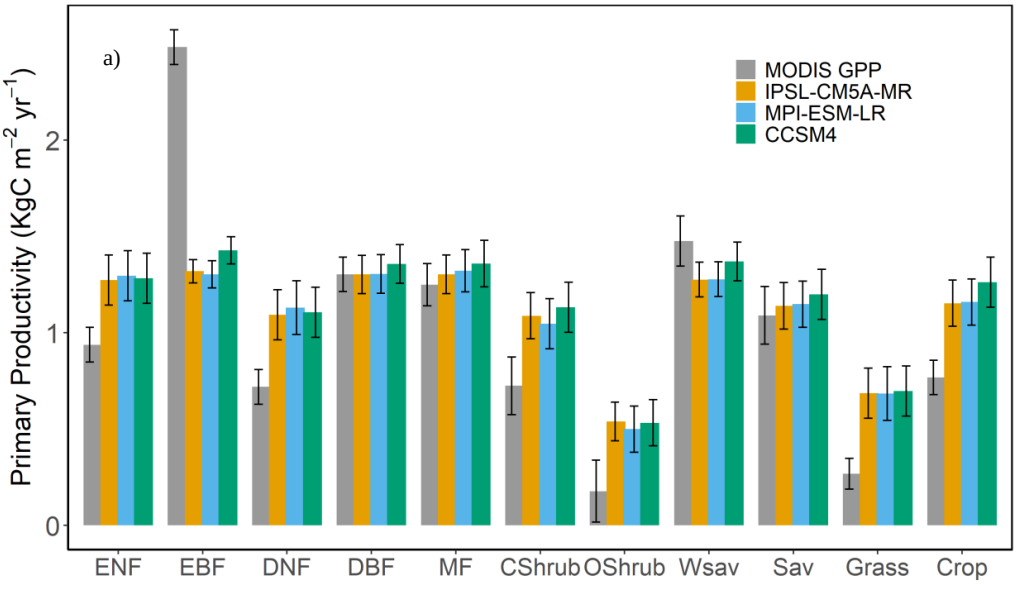

200

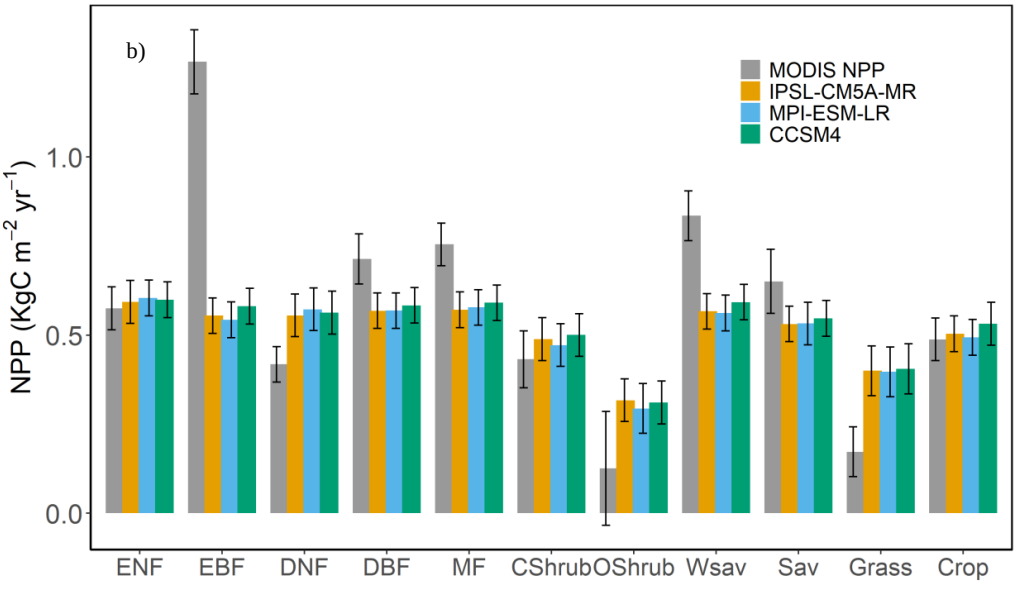

https://doi.org/10.5194/esd-2020-84
Preprint. Discussion started: 26 November 2020

Earth System Dynamics
Discussions
Open Access
EGU

Figure 7: (a) Mean MOD17 and LPJ-GUESS GPP per land cover class (b) Mean MOD17 and LPJ-GUESS NPP per land cover class. Vertical black bars illustrate ± standard error where *n*=11.

3.3 Projected Spatial Changes in the Pattern of NBP and VegC

The spatial maps for NBP shown in Figure 8 presents the averaged spatial NBP estimated for 1850-1950, 1951-2006 and 2006-2100 (RCP2.6 and RCP8.5) for CCSM4 respectively. The results of IPSL-CM5A-MR and MPI-ESM-LR are included in the supplementary information, as all three models showed a similar trend for both variables with minimal difference (Supplementary Figure S1 and Figure S2). The LPJ-GUESS mean NBP from 1850 to 1950 is 0.0011 kgC m^{-2} yr^{-1} and -0.0017 kgC m^{-2} yr^{-1} for 1951 to 2005. The simulations have shown a shift from carbon source to sink in both future scenarios with mean NBP of 0.0206 kg C m^{-2} yr^{-1} and 0.0466 kg C m^{-2} yr^{-1} for RCP2.6 and RCP8.5 respectively.

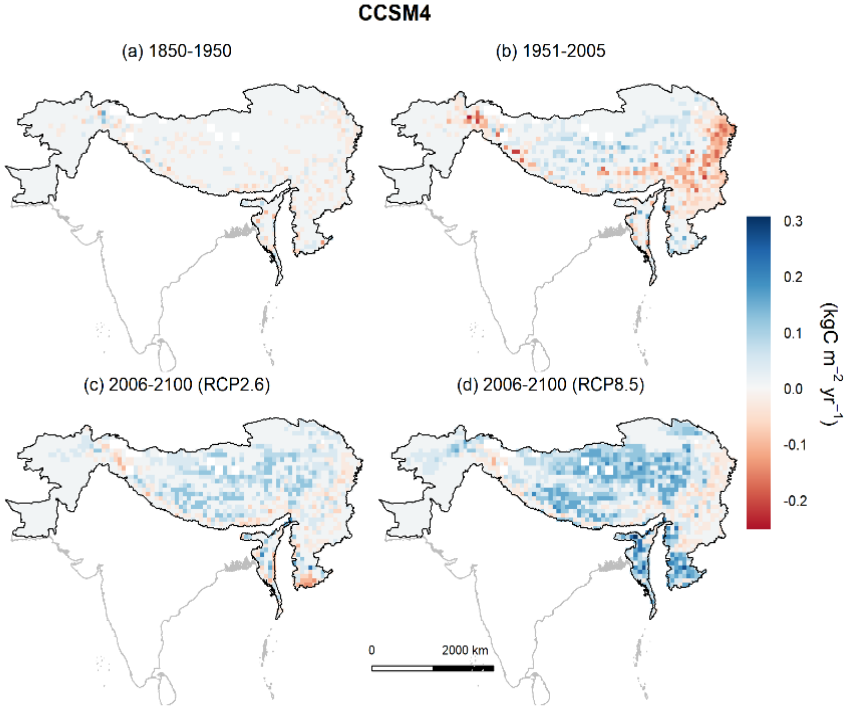

Figure 8: LPJ-GUESS simulated distribution by CCSM4 on NBP in HKH region under a) past period (1850-1950) b) present period (1951-2005) and future scenario under c) RCP2.6 scenario and d) RCP8.5.

https://doi.org/10.5194/esd-2020-84
Preprint. Discussion started: 26 November 2020

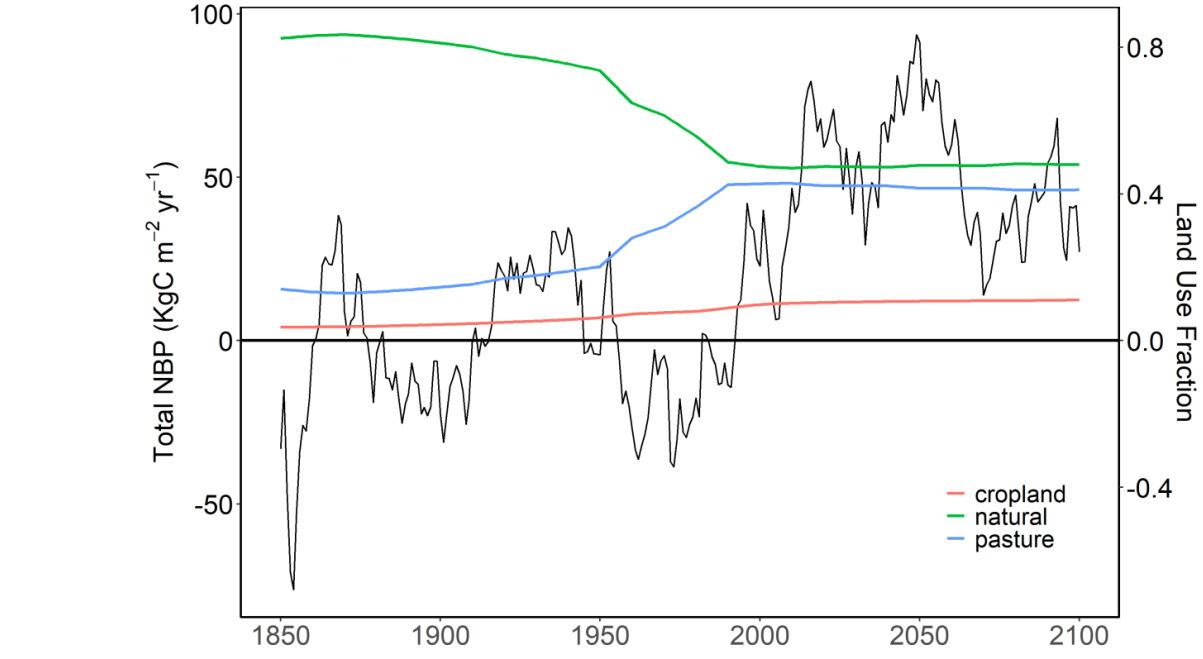

Figure 9: Total NBP as simulated by LPJ-GUESS RCP8.5 (CCSM4) is represented in black temporal line. The land use change fractions include cropland, natural vegetation and pasture denoted by blue, red (dashed) and green lines respectively.

The changes in land use fractions (cropland, pasture and natural vegetation) were also assessed in the HKH region with respect to NBP from 1850 to 2100 (Figure 9). The decline of natural vegetation through deforestation and conversion to croplands has resulted in carbon source for HKH for most part of mid-20th century and earlier 21st century. The simulations show a steady decline in NBP in the 1980s, as the natural vegetation fraction continue to decline and cropland and pasture land use fraction show a steady increase from 1850-2005.

The estimated total NBP for HKH region for the three CMIP5 models are shown in Figure 10. The temporal trend of total net biome productivity for the three CMIP5 models. In 1951-2005 (with respect to past period) MPI-ESM-LR and CCSM4 show a decreasing trend of total NBP, however IPSL show an increase for that time period. The average total NBP for RCP2.6 was estimated to be 55 kg C m^{-2} yr^{-1} and for RCP.8.5 it was 111 kg C m^{-2} yr^{-1}. All ESMs follow a similar pattern, showing a stronger carbon sink ability in RCP8.5. Previous research carried out by various authors have shed light on the driving factors that have caused HKH to act as a carbon source for the time period from 1951 to 2005. For instance (Pulakesh et al., 2017) have reported an increase in forest cover loss and high population increase during 2000-2010 in the HKH region. Furthermore (Behera et al., 2018b) reported deforestation in the major part of

https://doi.org/10.5194/esd-2020-84
Preprint. Discussion started: 26 November 2020

Earth System Dynamics Discussions
Open Access
EGU

northeast India from 1985-2005. The land use changes observed by various author in HKH are well reflected in LPJ-GUESS simulations of NBP and are in line with the modelled land use fraction.

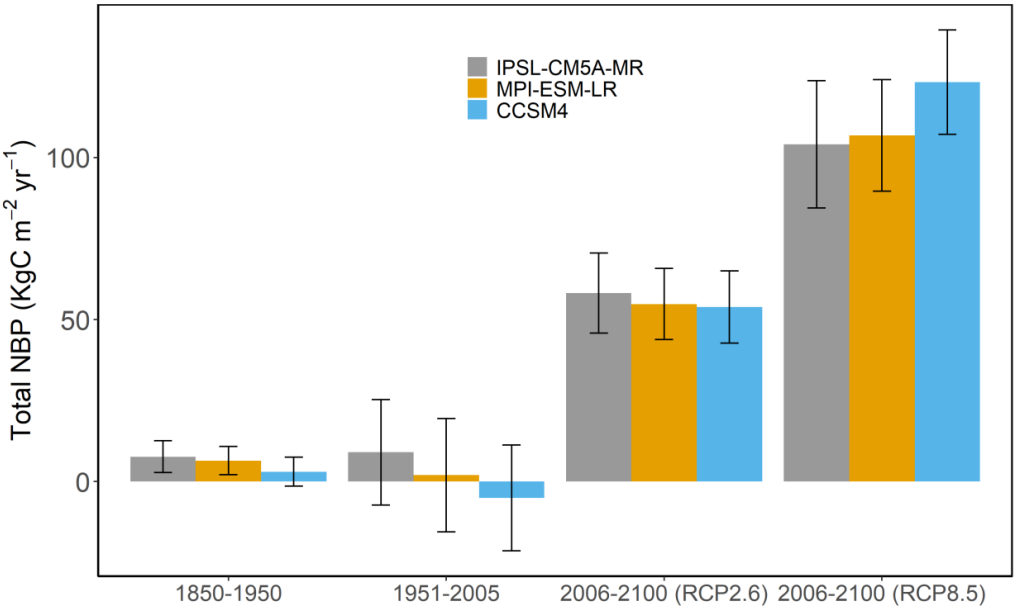

240

Figure 10: Model estimated total NBP for three time periods, 1850-1950, 1951-2005, 2006-2100 (RCP2.6) and 2006-2100 (RCP8.5) respectively. Error bars illustrate ± standard deviation where *n*=100 for 1850-1950, *n*=54 for 1951-2005 and *n*=94 for 2006-2100.

245 The total of VegC (Figure 11) was estimated for the HKH region, for three different time period 1850-1950, 1951-2005 and for future scenario 2006-2100 (RCP2.6 and RCP8.5) respectively. Model estimates of total VegC in HKH terrestrial ecosystems have increased since the 2005 and will increase under both future climate scenarios. The total VegC (averaged for all models) was estimated to be 7400 kg C m^{-2} by 1950, and by 2100, it is projected to range to 6000 kg C m^{-2} under the RCP2.6 scenario and 7600 kg C m^{-2} under the RCP8.5. Spatial patterns show that the mean
250 VegC (Figure 12) will increase most in the lower belt of the HKH region and north eastern region in HKH during 2006-2100 under the RCP2.6 an RCP8.5 scenarios. The spatial maps of IPSL-CM5A-MR and MPI-ESM-LR are provided in the supplementary information as the models showed a similar trend (Supplementary Figure S3 and Figure S4).

https://doi.org/10.5194/esd-2020-84
Preprint. Discussion started: 26 November 2020

Earth System Dynamics
Discussions
Open Access
EGU

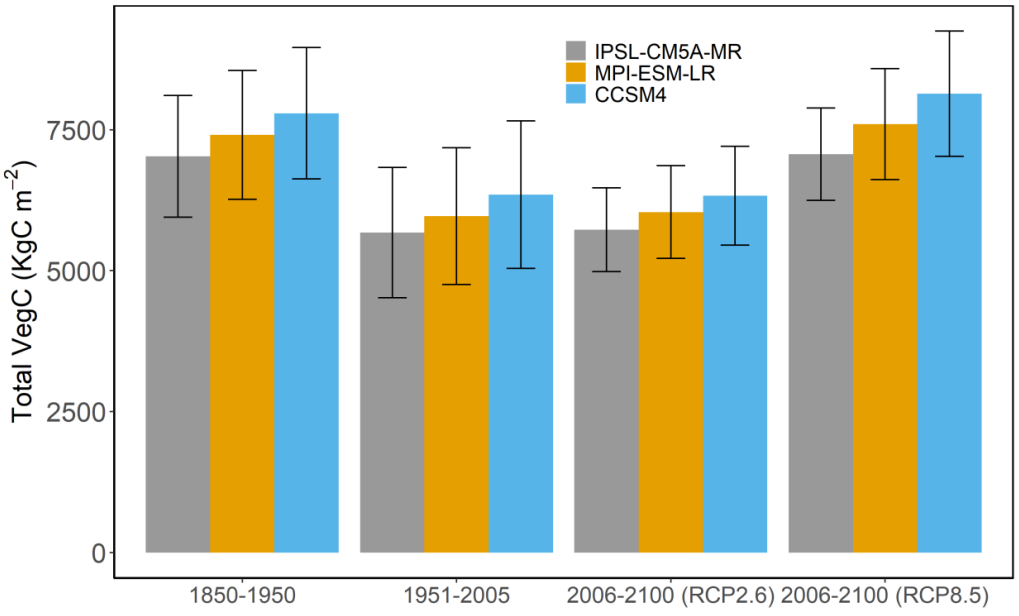

255 **Figure 11: The modeled trend of total VegC for HKH over the years 1850-2100. The future scenario is divided into RCP2.6 and RCP8.5. Vertical black bars illustrate ± standard error where *n*=100 for 1850-1950, *n*=54 for 1951-2005 and *n*=94 for 2006-2100.**

https://doi.org/10.5194/esd-2020-84
Preprint. Discussion started: 26 November 2020

Earth System Dynamics
Discussions
Open Access
EGU

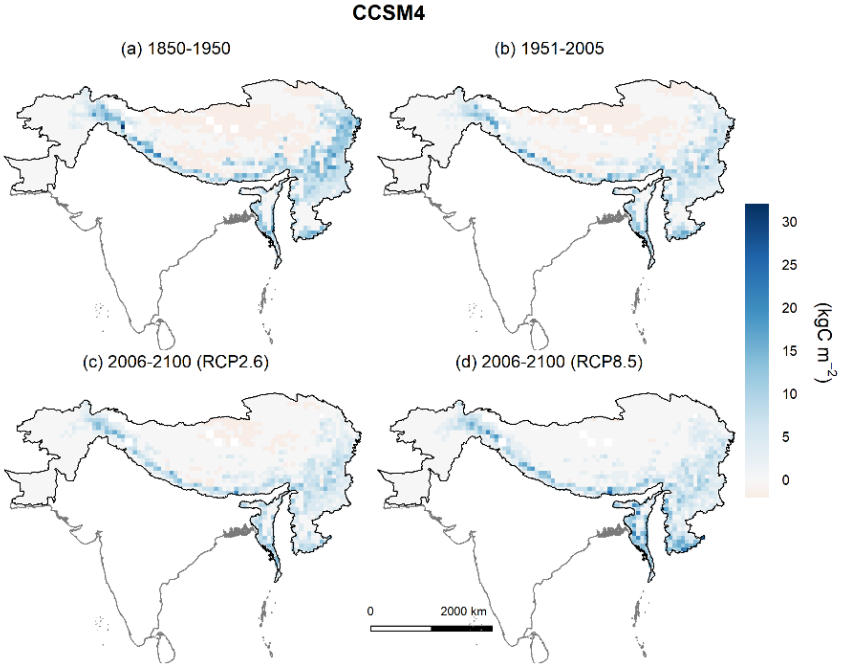

Figure 12: LPJ-GUESS simulated distribution by CCSM4 of VegC in HKH region under a) 1850-1950 b) 1951-2005 and future scenario under c) RCP2.6 scenario and d) RCP8.5.

4 Discussion

The global biomass datasets based on inventories and satellite observations have been recently available. For our first approach we compared the modelled simulations VegC and primary productivity with satellite observations. For VegC, the observed dataset is a global biomass map from the GEOCARBON project, a product of aboveground biomass dataset for the year 2000. A moderate agreement was found between GEOCARBON and IPSL-CM5A-MR forced simulated VegC and low agreement was found when climate data was supplied by MPI-ESM-LR and CCSM4. The difference between modelled and observed VegC may be attributed due to the differences in terms of the coverage of aboveground or belowground biomass of both datasets. The GEOCARBON dataset includes the spatial distribution of forest biomass covering only the aboveground vegetation for 2000. On the other hand, LPJ-GUESS simulation cover both above and belowground. Hence uncertainties may rise due to the converting aboveground biomass to the total of aboveground and belowground biomass for the datasets of GEOCARBON on order to be comparable with LPJ-GUESS VegC. Furthermore satellite-derived biomass dataset GEOCARBON was generated by harmonization of datasets of two different years. The tropical biomass products represent the year 2000 status of forests, and the boreal aboveground biomass maps are based on spaceborne radar data from the year 2010. The LPJ-GUESS VegC was

https://doi.org/10.5194/esd-2020-84
Preprint. Discussion started: 26 November 2020

averaged over the years from 1990 to 2015. Hence the difference in the years of observations might have introduced additional uncertainty. This drawback of observed dataset was also highlighted by (Li et al., 2017).

Secondly, we compared the LPJ-GUESS GPP and NPP with MODIS datasets from 2000-2010. A higher GPP and NPP emerged in areas covered with dense forests mainly in the southeast and southwest HKH region, especially in Bangladesh and Myanmar. The LPJ-GUESS GPP showed a better agreement with GPP MODIS than NPP MODIS. It is important to note that the DGVMs including LPJ-GUESS and the MODIS algorithm do not share a common meteorological drivers and that might be the potential to bring out a weak to moderate correlation between the two datasets (Liu et al., 2018). Previous literature have also reported that DGVMs generally overestimate GPP. Yet most of the researchers suggest that simulated GPP by DGVMs were neither overestimated nor underestimated, but the results are limited by number of observational or model abilities. For instance our modelled LPJ simulations have few important processes missing such as impact of nitrogen deposition (Li et al., 2016). The inconsistencies of primary productivity for EBF was also observed in various studies (Ardö, 2015; Garrigues et al., 2008). Areas affected by frequent cloud cover or atmospheric contamination may then show inconsistent estimates of vegetation productivity using MOD17 (or any method based on satellite based observations).

The second approach was to explore the variability of NBP and VegC over HKH from 1850-2100 and how this variability was influenced by factors of land use changes such as cropland, pastures and natural vegetation. Results showed that the terrestrial ecosystems of HKH had been a carbon sink for the period of 1850-1950 with a general positive NBP. There was a land use signal around 1950s where most of the fluctuation of NBP takes place. Since 1950s the land use fraction cropland and pasture began to increase while there was a reduction in net biome productivity.

Past literature based on modelling studies (Houghton et al., 1987) did capture a large net release of carbon in the 1980s from Nepal, Bangladesh, Bhutan, India, Pakistan, Myanmar and China due to land use change mainly deforestation. Extensive research has shed light on the serious degradation of grasslands on the Tibetan Plateau of China due to anthropogenic disturbances since the 1960s (Joshi et al., 2013;Wang et al., 2008). This degradation is well captured by the LPJ-GUESS simulation as a reduction of NBP in parts of China can be seen in the spatial maps from 1950-2005. Furthermore, a recent study carried out by (Calle et al., 2016) calculated the regional carbon fluxes LULCC in Asia for the period from 1980 to 2009, using eight carbon cycle DGVMs. Since the 1980s, the ensemble mean of the DGVMs also have shown a net source of South Asia and East Asia. From 1951 to 2005, most parts of the HKH underwent rapid population and economic growth increasing the demand for natural resources, hence resulting in large changes in LULCC and habitat fragmentation. However, LULCC can result in carbon source and carbon sink. (Lal, 2002) suggests that the balanced land use management can restore up to seventy percent of carbon that has been released to the atmosphere contributing to a reduction of carbon emissions.

https://doi.org/10.5194/esd-2020-84
Preprint. Discussion started: 26 November 2020

The LPJ-GUESS simulations for the HKH for 2006-2100 for both scenarios predicted a net sink of carbon. The simulations of LPJ-GUESS of HKH region was consistent with the previous studies carried out at a global scale where a net sink was reported in the future scenario by various DGVMs during the next century (Cramer et al., 2001). A greater increase in VegC and NBP was seen in RCP8.5, as rate of photosynthesis by terrestrial vegetation rises due to increase with atmospheric CO_2 content leading to increased carbon uptake. Global scale study carried out by (Thompson et al., 2004) discussed that the CO_2 fertilization could limit the global warming in the future scenario, however the nutrient limitations could weaken this effect. However, the version of LPJ-GUESS used in this study did not take account of nutrient limitations and assume nitrogen to be at an optimal level for the terrestrial vegetation. The coupling of carbon and nitrogen cycles are becoming widely recognized as nitrogen dynamics have been incorporated into global C cycling model (Fleischer et al., 2015). However there is large variation in the net effect on NBP and VegC due to uncertainties arising from different climatic forcing from respective ESMs and its description of future climate (Ahlström et al., 2017).

5 Conclusion

The results of the study has indicated that HKH will act as a net sink of C. However, the extent to which it will remain a C sink is uncertain as the parameterizations in LPJ-GUESS are in the early stages of validation and implementation in climate models. Uncertainties and large variation was found between the observed and modelled datasets. It is important to note that as long as obtainability and access of meteorological data at a regional level and in situ validation data such as eddy covariance measurements and long-term ecological field assessments remain scarce, it can be expected the representativity of vegetation carbon and vegetation productivity estimates for HKH to remain hard to evaluate and determine. The LPJ-GUESS simulations revealed that the NBP is projected to be higher in future scenario given that the LULCC remains stable. Furthermore VegC storage spatial and temporal analysis suggest that, for the RCP8.5 scenario, the CMIP5 ESMs produces, on average, a slightly higher VegC compared to the RCP2.6 attributing to the CO_2 fertilization effect. It is predicted the region will act as net sink of C in the future scenario. Vegetation fluxes can help to analyze the carbon storage patterns, however further studies are required to assess the effects of climatic changes and anthropogenic activities on the fragile ecosystems of the HKH for the establishment of policies to improve the livelihood of the local population and the overall carbon balance in the region.

Acknowledgements. The LPJ-GUESS data was provided by Anders Ahlström, Lund University. This work was supported by NUST Research Grant for MS students.

Data/Code Availability. Data used in this study is available on the 4TU.ResearchData.

Conflict of Interest. There is no conflict of interest.

https://doi.org/10.5194/esd-2020-84
Preprint. Discussion started: 26 November 2020


Earth System Dynamics Discussions

345 **References**

Ahlström, A., Schurgers, G., Arneth, A. and Smith, B.: Robustness and uncertainty in terrestrial ecosystem carbon response to CMIP5 climate change projections, Environ. Res. Lett., 7(4), doi:10.1088/1748-9326/7/4/044008, 2012.

Ahlström, A., Schurgers, G. and Smith, B.: The large influence of climate model bias on terrestrial carbon cycle simulations, Environ. Res. Lett., 12(1), 014004, doi:10.1088/1748-9326/12/1/014004, 2017.

350 Almeida, C. T. de, Delgado, R. C., Galvão, L. S., Aragão, L. E. de O. C. e. and Ramos, M. C.: Improvements of the MODIS Gross Primary Productivity model based on a comprehensive uncertainty assessment over the Brazilian Amazonia, ISPRS J. Photogramm. Remote Sens., 145, 268–283, doi:10.1016/j.isprsjprs.2018.07.016, 2018.

Anon: LP DAAC - AppEEARS, [online] Available from: https://lpdaac.usgs.gov/tools/appeears/ (Accessed 21 January 2020), n.d.

355 Ardö, J.: Comparison between remote sensing and a dynamic vegetation model for estimating terrestrial primary production of Africa, Carbon Balance Manag., 10(1), doi:10.1186/s13021-015-0018-5, 2015.

Behera, M. D., Murthy, M. S. R., Das, P. and Sharma, E.: Modelling forest resilience in Hindu Kush Himalaya using geoinformation, J. Earth Syst. Sci., 127(7), doi:10.1007/s12040-018-1000-x, 2018a.

Behera, M. D., Tripathi, P., Das, P., Srivastava, S. K., Roy, P. S., Joshi, C., Behera, P. R., Deka, J., Kumar, P., Khan,

360 M. L., Tripathi, O. P., Dash, T. and Krishnamurthy, Y. V. N.: Remote sensing based deforestation analysis in Mahanadi and Brahmaputra river basin in India since 1985, J. Environ. Manage., 206, 1192–1203, doi:10.1016/j.jenvman.2017.10.015, 2018b.

Burton J. Andrew, Melillo M. Jerry and Frey D. Serita: Adjustment of Forest Ecosystem Root Respiration as Temperature Warms, J. Integr. Plant Biol., 50(11), 1467–1483, 2008.

365 Calle, L., Canadell, J. G., Patra, P., Ciais, P., Ichii, K., Tian, H., Kondo, M., Piao, S., Arneth, A., Harper, A. B., Ito, A., Kato, E., Koven, C., Sitch, S., Stocker, B. D., Vivoy, N., Wiltshire, A., Zaehle, S. and Poulter, B.: Regional carbon fluxes from land use and land cover change in Asia, 1980-2009, Environ. Res. Lett., 11(7), 1–12, doi:10.1088/1748-9326/11/7/074011, 2016.

Cao, R., Shen, M., Zhou, J. and Chen, J.: Modeling vegetation green-up dates across the Tibetan Plateau by including

370 both seasonal and daily temperature and precipitation, Agric. For. Meteorol., 249, 176–186, doi:10.1016/j.agrformet.2017.11.032, 2018.

Chen, H., Zhu, Q., Peng, C., Wu, N., Wang, Y., Fang, X., Gao, Y., Zhu, D., Yang, G., Tian, J., Kang, X., Piao, S., Ouyang, H., Xiang, W., Luo, Z., Jiang, H., Song, X., Zhang, Y., Yu, G., Zhao, X., Gong, P., Yao, T. and Wu, J.: The impacts of climate change and human activities on biogeochemical cycles on the Qinghai-Tibetan Plateau, Glob.

375 Chang. Biol., 19(10), 2940–2955, doi:10.1111/gcb.12277, 2013.

Chettri, N., Shrestha, A. B. and Sharma, E.: Himalayan weather and climate and their impact on the environment, Himal. Weather Clim. their Impact Environ., (December 2019), 1–577, doi:10.1007/978-3-030-29684-1, 2019.

Cramer, W., Bondeau, A., Woodward, F. I., Prentice, I. C., Betts, R. A., Brovkin, V., Cox, P. M., Fisher, V., Foley, J. A., Friend, A. D., Kucharik, C., Lomas, M. R., Ramankutty, N., Sitch, S., Smith, B., White, A. and Young-Molling,

380 C.: Global response of terrestrial ecosystem structure and function to CO2 and climate change: Results from six dynamic global vegetation models, Glob. Chang. Biol., 7(4), 357–373, doi:10.1046/j.1365-2486.2001.00383.x, 2001.

https://doi.org/10.5194/esd-2020-84
Preprint. Discussion started: 26 November 2020

Das, P., Behera, M. D. and Murthy, M. S. R.: Forest fragmentation and human population varies logarithmically along elevation gradient in Hindu Kush Himalaya - utility of geospatial tools and free data set, J. Mt. Sci., 14(12), 2432–2447, doi:10.1007/s11629-016-4159-0, 2017.

Delpierre, N., Soudani, K., François, C., Köstner, B., Pontailler, J. Y., Nikinmaa, E., Misson, L., Aubinet, M., Bernhofer, C., Granier, A., Grünwald, T., Heinesch, B., Longdoz, B., Ourcival, J. M., Rambal, S., Vesala, T. and Dufrêne, E.: Exceptional carbon uptake in European forests during the warm spring of 2007: A data-model analysis, Glob. Chang. Biol., 15(6), 1455–1474, doi:10.1111/j.1365-2486.2008.01835.x, 2009.

Du, M., Kawashima, S., Yonemura, S., Zhang, X. and Chen, S.: Mutual influence between human activities and climate change in the Tibetan Plateau during recent years, in Global and Planetary Change, vol. 41, pp. 241–249., 2004.

Fleischer, K., Wårlind, D., Van Der Molen, M. K., Rebel, K. T., Arneth, A., Erisman, J. W., Wassen, M. J., Smith, B., Gough, C. M., Margolis, H. A., Cescatti, A., Montagnani, L., Arain, A. and Dolman, A. J.: Low historical nitrogen deposition effect on carbon sequestration in the boreal zone, J. Geophys. Res. Biogeosciences, 120(12), 2542–2561, doi:10.1002/2015JG002988, 2015.

Friedl, M. A., McIver, D. K., Hodges, J. C. F., Zhang, X. Y., Muchoney, D., Strahler, A. H., Woodcock, C. E., Gopal, S., Schneider, A., Cooper, A., Baccini, A., Gao, F. and Schaaf, C.: Global land cover mapping from MODIS: Algorithms and early results, Remote Sens. Environ., 83(1–2), 287–302, doi:10.1016/S0034-4257(02)00078-0, 2002.

Friedlingstein, P., Jones, M. W., O'Sullivan, M., Andrew, R. M., Hauck, J., Peters, G. P., Peters, W., Pongratz, J., Sitch, S., Le Quéré, C., DBakker, O. C. E., Canadell1, J. G., Ciais1, P., Jackson, R. B., Anthoni1, P., Barbero, L., Bastos, A., Bastrikov, V., Becker, M., Bopp, L., Buitenhuis, E., Chandra, N., Chevallier, F., Chini, L. P., Currie, K. I., Feely, R. A., Gehlen, M., Gilfillan, D., Gkritzalis, T., Goll, D. S., Gruber, N., Gutekunst, S., Harris, I., Haverd, V., Houghton, R. A., Hurtt, G., Ilyina, T., Jain, A. K., Joetzjer, E., Kaplan, J. O., Kato, E., Goldewijk, K. K., Korsbakken, J. I., Landschützer, P., Lauvset, S. K., Lefèvre, N., Lenton, A., Lienert, S., Lombardozzi, D., Marland, G., McGuire, P. C., Melton, J. R., Metzl, N., Munro, D. R., Nabel, J. E. M. S., Nakaoka, S. I., Neill, C., Omar, A. M., Ono, T., Peregon, A., Pierrot, D., Poulter, B., Rehder, G., Resplandy, L., Robertson, E., Rödenbeck, C., Séférian, R., Schwinger, J., Smith, N., Tans, P. P., Tian, H., Tilbrook, B., Tubiello, F. N., Van Der Werf, G. R., Wiltshire, A. J. and Zaehle, S.: Global carbon budget 2019, Earth Syst. Sci. Data, 11(4), 1783–1838, doi:10.5194/essd-11-1783-2019, 2019.

Garrigues, S., Lacaze, R., Baret, F., Morisette, J. T., Weiss, M., Nickeson, J. E., Fernandes, R., Plummer, S., Shabanov, N. V., Myneni, R. B., Knyazikhin, Y. and Yang, W.: Validation and intercomparison of global Leaf Area Index products derived from remote sensing data, J. Geophys. Res. Biogeosciences, 113(2), doi:10.1029/2007JG000635, 2008.

Houghton, R. A., Boone, R. D., Fruci, J. R., Hobbi, J. E., Melillo, J. M., Palm, C. A., Peterson, B. J., Shaver, G. R., Woodwell, G. M., Moore, B., Skole, D. L. and Myers, N.: The flux of carbon from terrestrial ecosystems to the atmosphere in 1980 due to changes in land use: geographic distribution of the global flux, Tellus B, 39 B(1–2), 122–139, doi:10.1111/j.1600-0889.1987.tb00277.x, 1987.

Hurtt, G. C., Chini, L. P., Frolking, S., Betts, R. A., Feddema, J., Fischer, G., Fisk, J. P., Hibbard, K., Houghton, R.

https://doi.org/10.5194/esd-2020-84
Preprint. Discussion started: 26 November 2020

A., Janetos, A., Jones, C. D., Kindermann, G., Kinoshita, T., Klein Goldewijk, K., Riahi, K., Shevliakova, E., Smith, S., Stehfest, E., Thomson, A., Thornton, P., van Vuuren, D. P. and Wang, Y. P.: Harmonization of land-use scenarios for the period 1500-2100: 600 years of global gridded annual land-use transitions, wood harvest, and resulting secondary lands, Clim. Change, 109(1), 117–161, doi:10.1007/s10584-011-0153-2, 2011.

Joshi, L., Shrestha, R. M., Jasra, A. W., Joshi, S., Gilani, H. and Ismail, M.: Rangeland Ecosystem Services in the Hindu Kush Himalayan Region. In Ning, Wu; Rawat, GS; Joshi, S; Ismail, M; Sharma, E (2013) High-altitude rangelands and their interfaces in the Hindu Kush Himalayas. Kathmandu: ICIMOD, 2013.

Kondo, M., Ichii, K., Patra, P. K., Poulter, B., Calle, L., Koven, C., Pugh, T. A. M., Kato, E., Harper, A., Zaehle, S. and Wiltshire, A.: Plant Regrowth as a Driver of Recent Enhancement of Terrestrial CO_2 Uptake, Geophys. Res. Lett., 45(10), 4820–4830, doi:10.1029/2018GL077633, 2018.

Krishnan, R., Shrestha, A. B., Ren, G., Rajbhandari, R., Saeed, S., Sanjay, J., Syed, M. A., Vellore, R., Xu, Y., You, Q. and Ren, Y.: Unravelling Climate Change in the Hindu Kush Himalaya: Rapid Warming in the Mountains and Increasing Extremes, in The Hindu Kush Himalaya Assessment, pp. 57–97, Springer International Publishing., 2019.

Lal, R.: Soil carbon dynamics in cropland and rangeland, in Environmental Pollution, vol. 116, pp. 353–362., 2002.

Li, W., Ciais, P., Peng, S., Yue, C., Wang, Y., Thurner, M., Saatchi, S. S., Arneth, A., Avitabile, V., Carvalhais, N., Harper, A. B., Kato, E., Koven, C., Liu, Y. Y., Nabel, J. E. M. S., Pan, Y., Pongratz, J., Poulter, B., Pugh, T. A. M., Santoro, M., Sitch, S., Stocker, B. D., Viovy, N., Wiltshire, A., Yousefpour, R. and Zaehle, S.: Land-use and land-cover change carbon emissions between 1901 and 2012 constrained by biomass observations, Biogeosciences, 14, 5053–5067, doi:10.5194/bg-14-5053-2017, 2017.

Li, X., Zhu, Z., Zeng, H. and Piao, S.: Estimation of gross primary production in China (1982-2010) with multiple ecosystem models Legacy effects of drought on gross primary productivity of temperate grassland in China View project Estimation of gross primary production in China (1982-2010) with multiple ecosystem models, Ecol. Modell., 324, 33–44, doi:10.1016/j.ecolmodel.2015.12.019, 2016.

Liu, L., Peng, S., AghaKouchak, A., Huang, Y., Li, Y., Qin, D., Xie, A. and Li, S.: Broad Consistency Between Satellite and Vegetation Model Estimates of Net Primary Productivity Across Global and Regional Scales, J. Geophys. Res. Biogeosciences, 123(12), 3603–3616, doi:10.1029/2018JG004760, 2018.

Phillips, O. L. and Lewis, S. L.: Evaluating the tropical forest carbon sink, Glob. Chang. Biol., 20(7), 2039–2041, doi:10.1111/gcb.12423, 2014.

Pugh, T. A. M., Jones, C. D., Huntingford, C., Burton, C., Arneth, A., Brovkin, V., Ciais, P., Lomas, M., Robertson, E., Piao, S. L. and Sitch, S.: A Large Committed Long-Term Sink of Carbon due to Vegetation Dynamics, Earth's Futur., 6(10), 1413–1432, doi:10.1029/2018EF000935, 2018.

Pugh, T. A. M., Lindeskog, M., Smith, B., Poulter, B., Arneth, A., Haverd, V. and Calle, L.: Role of forest regrowth in global carbon sink dynamics, Proc. Natl. Acad. Sci. U. S. A., 116(10), 4382–4387, doi:10.1073/pnas.1810512116, 2019.

Pulakesh, D., Mukunda Dev, B. and Manchiraju Sri Ramachandra, M.: Forest fragmentation and human population varies logarithmically along elevation gradient in Hindu Kush Himalaya-utility of geospatial tools and free data set, J. Mt. Sci, 14(12), 2432–2447, doi:10.1007/s11629-016-4159-0, 2017.

https://doi.org/10.5194/esd-2020-84
Preprint. Discussion started: 26 November 2020


Earth System Dynamics Discussions

Riahi, K., Rao, S., Krey, V., Cho, C., Chirkov, V., Fischer, G., Kindermann, G., Nakicenovic, N. and Rafaj, P.: RCP 8.5-A scenario of comparatively high greenhouse gas emissions, Clim. Change, 109(1), 33–57, doi:10.1007/s10584-011-0149-y, 2011.

Saatchi, S. S., Harris, N. L., Brown, S., Lefsky, M., Mitchard, E. T. A., Salas, W., Zutta, B. R., Buermann, W., Lewis, S. L., Hagen, S., Petrova, S., White, L., Silman, M. and Morel, A.: Benchmark map of forest carbon stocks in tropical regions across three continents, Proc. Natl. Acad. Sci. U. S. A., 108(24), 9899–9904, doi:10.1073/pnas.1019576108, 2011.

Sitch, S., Friedlingstein, P., Gruber, N., Jones, S. D., Murray-Tortarolo, G., Ahlström, A., Doney, S. C., Graven, H., Heinze, C., Huntingford, C., Levis, S., Levy, P. E., Lomas, M., Poulter, B., Viovy, N., Zaehle, S., Zeng, N., Arneth, A., Bonan, G., Bopp, L., Canadell, J. G., Chevallier, F., Ciais, P., Ellis, R., Gloor, M., Peylin, P., Piao, S. L., Le Quéré, C., Smith, B., Zhu, Z. and Myneni, R.: Recent trends and drivers of regional sources and sinks of carbon dioxide, Biogeosciences, 12(3), 653–679, doi:10.5194/bg-12-653-2015, 2015.

Smith, B., Prentice, I. C. and Sykes, M. T.: Representation of vegetation dynamics in modelling of European ecosystems: comparison of two contrasting approaches, Glob. Ecol. Biogeogr., 10, 621–637, doi:10.1046/j.1466-822X.2001.t01-1-00256.x, 2001.

Stocker, T. F., Qin, D., Plattner, G. K., Tignor, M. M. B., Allen, S. K., Boschung, J., Nauels, A., Xia, Y., Bex, V. and Midgley, P. M.: Climate change 2013 the physical science basis: Working Group I contribution to the fifth assessment report of the intergovernmental panel on climate change, Cambridge University Press., 2013.

Sullivan, P. F., Arens, S. J. T., Chimner, R. A. and Welker, J. M.: Temperature and microtopography interact to control carbon cycling in a high arctic fen, Ecosystems, 11(1), 61–76, doi:10.1007/s10021-007-9107-y, 2008.

Thompson, S. L., Govindasamy, B., Mirin, A., Caldeira, K., Delire, C., Milovich, J., Wickett, M. and Erickson, D.: Quantifying the effects of CO2-fertilized vegetation on future global climate and carbon dynamics, Geophys. Res. Lett., 31(23), 1–4, doi:10.1029/2004GL021239, 2004.

Todd-Brown, K. E. O., Randerson, J. T., Hopkins, F., Arora, V., Hajima, T., Jones, C., Shevliakova, E., Tjiputra, J., Volodin, E., Wu, T., Zhang, Q. and Allison, S. D.: Changes in soil organic carbon storage predicted by Earth system models during the 21st century, Biogeosciences, 11, 2341–2356, doi:10.5194/bg-11-2341-2014, 2014.

Trenberth, K. E., Dai, A., Schrier, G. van der, Jones, P. D., Barichivich, J., Briffa, K. R. and Sheffield, J.: Global warming and changes in drought, Nat. Clim. Chang. 2014 41, 4(1), 17–22, doi:10.1038/nclimate2067, 2013.

Urban, J., Ingwers, M. W., McGuire, M. A. and Teskey, R. O.: Increase in leaf temperature opens stomata and decouples net photosynthesis from stomatal conductance in Pinus taeda and Populus deltoides x nigra, J. Exp. Bot., 68(7), 1757–1767, doi:10.1093/jxb/erx052, 2017.

Van Vuuren, D. P., Den Elzen, M. G. J., Lucas, P. L., Eickhout, B., Strengers, B. J., Van Ruijven, B., Wonink, S. and Van Houdt, R.: Stabilizing greenhouse gas concentrations at low levels: An assessment of reduction strategies and costs, Clim. Change, 81(2), 119–159, doi:10.1007/s10584-006-9172-9, 2007.

Wang, H., Zhou, X., Wan, C., Fu, H., Zhang, F. and Ren, J.: Eco-environmental degradation in the northeastern margin of the Qinghai-Tibetan Plateau and comprehensive ecological protection planning, Environ. Geol., 55(5), 1135–1147, doi:10.1007/s00254-007-1061-7, 2008.

https://doi.org/10.5194/esd-2020-84
Preprint. Discussion started: 26 November 2020

Williams, A. P., Allen, C. D., Macalady, A. K., Griffin, D., Woodhouse, C. A., Meko, D. M., Swetnam, T. W., Rauscher, S. A., Seager, R., Grissino-Mayer, H. D., Dean, J. S., Cook, E. R., Gangodagamage, C., Cai, M. and
495 Mcdowell, N. G.: Temperature as a potent driver of regional forest drought stress and tree mortality, Nat. Clim. Chang., 3(3), 292–297, doi:10.1038/nclimate1693, 2013.

Wu, Z., Dijkstra, P., Koch, G. W., Peñuelas, J. and Hungate, B. A.: Responses of terrestrial ecosystems to temperature and precipitation change: A meta-analysis of experimental manipulation, Glob. Chang. Biol., 17(2), 927–942, doi:10.1111/j.1365-2486.2010.02302.x, 2011.

500 Zhao, M. and Running, S. W.: Drought-induced reduction in global terrestrial net primary production from 2000 through 2009, Science (80-.)., 329(5994), 940–943, doi:10.1126/science.1192666, 2010.

505